

# The Unified Tracking Controller for a Tilt-Rotor Unmanned Aerial Vehicle Based on the Dual Quaternion

Liuchao Jin

*Department of Mechanical Engineering  
Sichuan University - Pittsburgh Institute  
Chengdu, China  
liuchao.jin@link.cuhk.edu.hk*

Lu-An Chen

*Department of Mechanical Engineering  
Sichuan University - Pittsburgh Institute  
Chengdu, China  
luanchen@zju.edu.cn*

Yuchen Lou

*Department of Mechanical Engineering  
Sichuan University - Pittsburgh Institute  
Chengdu, China  
louyuchen@sjtu.edu.cn*

Qi Lu\*

*Department of Mechanical Engineering  
Sichuan University - Pittsburgh Institute  
Chengdu, China  
qi.lu@scupi.cn*

**Abstract**—Tilt-rotor multi-rotor UAV is a rapidly expanding field of research due to its benefits of full actuation, high force and torque capabilities, and great efficiency of hovering. The current controllers of tilt-rotor multi-rotor UAVs are primarily based on the Cartesian coordinate system to describe the position combined with the classical Euler angle approach, the direction cosine matrix or the quaternion to represent the attitude, which makes control lose its mathematical simplicity and has some singularity cases. In this paper, the system modelling of a tilt-rotor multi-rotor UAV using the unit dual quaternion is presented and a novel PID feedback linearization tracker is proposed. The developed controller has advantages of singularity free, attitude/position coupled motion tracking, and robustness to external disturbance. Applying the Laplace transform, the stability analysis is conducted by analyzing the poles and zeros of the closed-loop system. Simulation studies including the 6 DoF trajectory tracking and disturbance rejection are also performed to demonstrate the effectiveness of the proposed method. The simulation results illustrate that the proposed PID feedback linearization tracker has good tracking performance for both position and attitude and strong robustness against disturbance.

**Keywords**—Tilt-Rotor Multi-Rotor UAV, Unit Dual Quaternion, Feedback Linearization, Robot Dynamics and Control

## I. INTRODUCTION

In the last few decades, Unmanned Aerial Vehicles (UAVs) have developed rapidly and become increasingly widely used in various application scenarios due to their superior adaptability, survivability, and relatively low cost. Among various types of UAVs, tilt-rotor multi-rotor UAVs are special kinds of rotor UAVs. They have six independently controllable Degrees of Freedom (DoF), indicating that these kinds of UAVs are force-omnidirectional, which means the translational and rotational dynamics of the system are decoupled and they are fully actuated systems in any hover configuration. These special properties of tilt-rotor multi-rotor UAVs permit stable interaction with the environment, subvert the under-actuated deficiencies of conventional fixed-wing and fixed-rotor UAVs,

and provide compelling solutions for future applications in aerial robotics [1]. The force-omnidirectionality feature of tilt-rotor multi-rotor UAVs empowers them with the capability of complete attitude-omnidirectionality, allowing for unrestricted aerial motion and reliable tracking of 6 DoF trajectories. These superiorities of tilt-rotor multi-rotor UAVs contribute unique advantages to aerial photography, industrial inspection, and interactive applications, where motion and operation need to be achieved in confined space environments.

In the currently-studied controllers for tilt-rotor multi-rotor UAVs, utilizing the Cartesian coordinate system to describe the position combined with the classical Euler angle approach, the direction cosine matrix (DCM) or the quaternion to indicate the attitude is the most general motion description methods. The Euler angle method is preferred and commonly used because of its intuitiveness [1]–[5]. However, using the Euler angle representation will introduce the discontinuity [6] and also the singularity, i.e., gimbal lock—a phenomenon where one of the rotation axes aligns with the other axis [7], leading to the loss of one degree of freedom [8], which makes the control system generate improper control commands. The DCM is not affected by singularities and also has linear dynamics [9] so it is widely used in many controllers for tilt-rotor multi-rotor UAVs [10]–[13]. Nevertheless, the DCM and Cartesian coordinate system description used by these controllers have one  $3 \times 3$  matrix and one three-element vector, i.e., 12 elements, to be integrated, which leads to the excessive computational burden [14]. Compared with the DCM representation, the expression of quaternion for describing the attitude is more compact and it also doesn't have the singularity case suffered by the Euler angle representation. In the controllers of tilt-rotor multi-rotor UAVs, the quaternion is also often used to describe the orientation [15]–[18]. However, the quaternion-Cartesian coordinate representation that is used by tilt-rotor multi-rotor UAVs controllers has the characteristic that the position and attitude descriptions are not unified, which makes the platform model lose its mathematical simplicity. A computationally simpler and more stable mathematical tool for modelling

\* Corresponding Author

This work has been supported by the National Natural Science Foundation of China (Grant No. 62103291).

position and attitude tracking of tilt-rotor multi-rotor UAVs is the unit dual quaternion. A unit dual quaternion is made up of a unit quaternion and a translation vector based on Plück coordinates. Different from the unit quaternion, the unit dual quaternion represents not only the attitude change but also the positional movement of the rigid body, using only eight numbers with two constraints. The unit dual quaternion has been widely used in various fields in the past ten years due to its advantages of compact, unambiguity, singularity-free, and computational minimalistic rigid transform.

In recent years, the position and attitude tracking problem of rigid bodies and the control problem of UAVs including fixed-wing and quad-rotor types based on dual quaternion have been studied. According to the characteristics of the unit dual quaternion, Wang & Yu proposed a unit-dual-quaternion-based proportional-integral-derivative (PID) control scheme for the rigid-body transformation in 6 DoF and simulated on a quadrotor [19]. However, they only considered the kinematic control but did not introduce dynamics into its design. Based on the features of the unit dual quaternion, Wang & Yu also gave a general solution for the rigid body position and attitude tracking problem in a 3D space, and designed a PD unit-dual-quaternion-based tracker [20]. Nevertheless, this tracker cannot effectively compensate for uncertainty and external disturbance. Carino et al. presented the design and practical implementation of a quaternion control method to globally stabilize a quad-rotor UAV [21]. Using the PD control method, Abaunza et al. designed a quadcopter control law that utilized dual quaternions in an under-actuated system [22]. The above research is almost aimed at the exploration of the application of the dual quaternion to underactuated systems such as fixed-wing or quad-rotor UAVs. However, there is little research on the control of tilt-rotor multi-rotor UAVs based on the unit dual quaternion. Tilt-rotor multi-rotor UAVs is the type of UAVs that needs the unit dual quaternion more since they have the characteristics of attitude-omnidirectionality.

The main contributions of this paper are summarized as follows.

- In this paper, a novel PID feedback linearization tracker based on the unit dual quaternion is proposed for the tilt-rotor multi-rotor UAVs. In contrast to the PID control scheme proposed by [19], the designed PID feedback linearization tracker takes into account the characteristics and dynamics of tilt-rotor multi-rotor UAVs. In comparison to the PD feedback linearization tracker in [20], the proposed PID tracker can realize real-time tracking of the trajectory and attitude better and eliminate the tracking error using the integral term to make the tilt-rotor multi-rotor UAV system always stable. Different from the controller for tilt-rotor multi-rotor UAV in [1], the designed PID feedback linearization tracker based on unit dual quaternion can eliminate all singularity cases and discontinuities in the entire control system for the tilt-rotor multi-rotor UAV.
- The control allocation algorithm is improved to solve the discontinuities experienced in [2], which allows the tilt-

rotor multi-rotor UAV system to be more controllable.

The remainder of this paper is organized as follows. In Section II, the mathematical preliminaries of the unit dual quaternion are demonstrated, and the system modeling of the dynamics and kinematics for tilt-rotor multi-rotor UAVs based on unit dual quaternion is derived. Then, a novel PID feedback linearization tracker based on the unit dual quaternion is proposed in Section III. Section IV presents the simulation results of the designed tracker. Finally, the conclusion, as well as some discussions of the future work, is given in Section V.

## II. DUAL QUATERNION-BASED SYSTEM DYNAMICS

### A. Mathematical Preliminaries for Dual Quaternion

A regular dual number is expressed as  $\hat{s} = r + d\epsilon$  and consists of two components: the real part  $r$  and the dual part  $d$ , which can also be written as  $\hat{s} = [r, d]$ .  $\epsilon$  is the dual operator, a dimension unit vector perpendicular to the real number field  $\mathbb{R}$ , which satisfies  $\epsilon^2 = 0$  [23]. A quaternion space,  $\mathbb{H}$ , is defined as the real algebra generated by the four elements, 1,  $i$ ,  $j$ , and  $k$ , which has the form of  $q = s + (v_1i + v_2j + v_3k)$  [24].

A dual quaternion is an algebraic form that combines the dual number and the quaternion. It has the form of  $\hat{q} = q_r + q_d\epsilon$ , where  $q_r$  and  $q_d$  are all quaternions. Each dual quaternion is composed of eight components or two quaternions. Compared with the unit quaternion which can only denote rotation, the unit dual quaternion can describe both translation and rotation at the same time.

Some fundamental arithmetic operations of dual quaternions are shown here:

- Scalar Multiplication:  $s\hat{q} = sq_r + sq_d\epsilon$
- Addition:  $\hat{q}_1 + \hat{q}_2 = q_{r1} + q_{r2} + (q_{d1} + q_{d2})\epsilon$
- Multiplication:  $\hat{q}_1 \circ \hat{q}_2 = q_{r1} \circ q_{r2} + (q_{r1} \circ q_{d2} + q_{d1} \circ q_{r2})\epsilon$
- Conjugate:  $\hat{q}^* = q_r^* + q_d^*\epsilon$
- Magnitude:  $\|\hat{q}\|^2 = \hat{q} \circ \hat{q}^*$

where the operator ‘ $\circ$ ’ is (dual) quaternion multiplication. The unit condition for the dual quaternion is  $\|\hat{q}\| = 1$ , which can be also represented as  $q_r^*q_d + q_d^*q_r = 1$ . The dual quaternion can be utilized to describe translation and rotation synchronously in 3D space. A motion with a rotation  $q$  followed by a translation  $p^b$  or  $p^s$  can be described by

$$\hat{q} = q + \frac{\epsilon}{2}q \circ p^b = q + \frac{\epsilon}{2}p^s \circ q \quad (1)$$

where  $p^b$  and  $p^s$  are the translation motion in the body and spatial frame, respectively.

The logarithmic mapping of the dual quaternion can be represented as  $\ln \hat{q} = \frac{1}{2}(\theta + \epsilon p^b)$ , which is a dual vector quaternion [25].

The adjoint transformation of dual quaternion is given as:

$$Ad_{\hat{q}}\hat{V} = \hat{q} \circ \hat{V} \circ \hat{q}^{-1} = \hat{q} \circ \hat{V} \circ \hat{q}^* \quad (2)$$

Similar to the dual vector, the dual vector quaternion is the dual quaternion with the scalar part equal to 0, denoted as  $\hat{v} = [\hat{0}, \hat{v}]$ . And the dot-product of the dual vector quaternion is defined as (3).

$$\hat{k} \cdot \hat{v} = [0, K_r v_r] + \epsilon [0, K_d v_d] \quad (3)$$

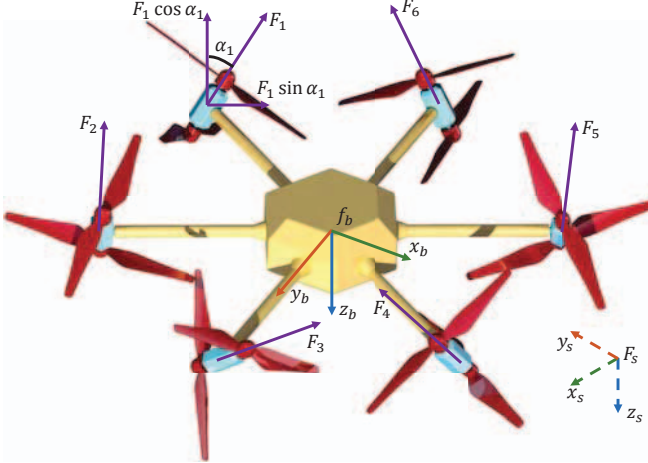


Fig. 1. System modeling of the tilt-rotor multi-rotor UAV.

where  $K_r$  and  $K_d$  are  $3 \times 3$  diagonal matrices with diagonal entries  $k_{r1}, k_{r2}, k_{r3}$  and  $k_{d1}, k_{d2}, k_{d3}$ , respectively, denoted as  $K_r = \text{diag}(k_{r1}, k_{r2}, k_{r3})$  and  $K_d = \text{diag}(k_{d1}, k_{d2}, k_{d3})$ .  $\text{diag}(\cdot)$  creates a matrix whose diagonal elements are equal to the corresponding diagonal elements  $(\cdot)$ .

### B. System Dynamics Based on Dual Quaternion

The system dynamics of tilt-rotor multi-rotor UAVs as shown in Fig. 1 is derived from the Newton-Euler approach in this subsection, which can be described by its translational and rotational dynamics, resulting in (4) [26].

$$\begin{cases} m\ddot{\mathbf{p}}^b = \mathbf{f} \\ J\dot{\boldsymbol{\omega}}^b + \boldsymbol{\omega}^b \times (J\boldsymbol{\omega}^b) = \boldsymbol{\tau} \end{cases} \quad (4)$$

After applying  $\dot{\hat{q}} = \hat{q} + \frac{\epsilon}{2}\hat{q} \circ \mathbf{p}^b$  to describe the translation  $\mathbf{p}^b$  after the rotation  $\hat{q}$ , and denoting linear and angular velocities of  $\dot{\mathbf{p}}^b$  and  $\boldsymbol{\omega}^b$ , respectively, the dynamics of a tilt-rotor multi-rotor UAV expressed with the unit dual quaternion is shown in (5), (6), and (7) [20].

$$\dot{\hat{q}} = \frac{1}{2}\hat{q} \circ \boldsymbol{\xi}^b \quad (5)$$

$$\boldsymbol{\xi}^b = \boldsymbol{\omega}^b + \epsilon(\dot{\mathbf{p}}^b + \boldsymbol{\omega}^b \times \mathbf{p}^b) \quad (6)$$

$$\dot{\boldsymbol{\xi}}^b = \hat{\mathbf{F}} + \hat{\mathbf{U}} \quad (7)$$

where  $\hat{\mathbf{F}}$  and  $\hat{\mathbf{U}}$  can be represented by (8) ( $\mathbf{a} = -J^{-1}\boldsymbol{\omega}^b \times J\boldsymbol{\omega}^b$ ).

$$\begin{cases} \hat{\mathbf{F}} = \mathbf{a} + \epsilon(\mathbf{a} \times \mathbf{p}^b + \boldsymbol{\omega}^b \times \dot{\mathbf{p}}^b) \\ \hat{\mathbf{U}} = J^{-1}\boldsymbol{\tau} + \epsilon(\mathbf{f}/m + J^{-1}\boldsymbol{\tau} \times \mathbf{p}^b) \end{cases} \quad (8)$$

### III. CONTROLLER DESIGN

The proposed control structure for a tilt-rotor multi-rotor UAV is drawn in the block diagram shown in Fig. 2. For the remainder of this section, the details of the controller development are discussed.

#### A. Error Dynamics Based on Dual Quaternion

The left-invariant error is denoted as the tracking error between the actual configuration  $\hat{q}$  and the desired configuration  $\hat{q}_d$ , as shown in (9), for the trajectory tracking [20].

$$\hat{q}_e = \hat{q}_d^* \circ \hat{q} \quad (9)$$

After some algebraic operations,  $\dot{\hat{q}}_e$  can be rewritten into a form similar to (5) as follows:

$$\dot{\hat{q}}_e = \frac{1}{2}\hat{q}_e \circ \boldsymbol{\xi}_e^b \quad (10)$$

where

$$\boldsymbol{\xi}_e^b = \boldsymbol{\xi}^b - Ad_{\hat{q}_e^*} \boldsymbol{\xi}_d^b \quad (11)$$

$\boldsymbol{\xi}_e^b$  can also be represented as (12)

$$\boldsymbol{\xi}_e^b = [0, \boldsymbol{\omega}_e^b] + \epsilon[0, \mathbf{p}_e^b + \boldsymbol{\omega}_e^b \times \mathbf{p}_e^b] \quad (12)$$

Differentiating (12) and also substituting  $\boldsymbol{\omega}_e^b = \dot{\theta}_e^b$  into it give that

$$\dot{\boldsymbol{\xi}}_e^b = [0, \ddot{\theta}_e^b] + \epsilon[0, \ddot{\mathbf{p}}_e^b + \ddot{\theta}_e^b \times \mathbf{p}_e^b + \dot{\theta}_e^b \times \dot{\mathbf{p}}_e^b] \quad (13)$$

Also, differentiating (11) obtains that

$$\dot{\boldsymbol{\xi}}_e^b = \dot{\boldsymbol{\xi}}^b - Ad_{\hat{q}_e^*} \dot{\boldsymbol{\xi}}_d^b - [\hat{0}, Ad_{\hat{q}_e^*} \boldsymbol{\xi}_d^b \times \boldsymbol{\xi}_e^b] \quad (14)$$

#### B. Tracker Design and Stability Analysis

This work proposes a controller structure using the feedback linearization principle:

$$\begin{aligned} \hat{\mathbf{U}} &= \text{PID feedback} \\ &\quad + \text{feedforward compensation} \end{aligned} \quad (15)$$

In (15), feedforward compensation is utilized to eliminate nonlinearity [20], and PID feedback is to ensure stability, eliminate the steady-state error, and reject the disturbance. In this subsection, a stable feedback linearization tracker based on this general structure is proposed.

Following this structure, a novel PID feedback linearization tracker is designed based on the dual quaternion Lie-group and its Lie-algebra associated with its logarithmic mapping. The controller is shown in (16).

$$\begin{aligned} \hat{\mathbf{U}} = -2 &\left( \hat{k}_p \cdot \ln \hat{q}_e + \hat{k}_i \cdot \int_0^t \ln \hat{q}_e dt + \hat{k}_d \cdot (\ln \hat{q}_e)' \right) - \hat{\mathbf{F}} \\ &+ Ad_{\hat{q}_e^*} \dot{\boldsymbol{\xi}}_d^b + [\hat{0}, Ad_{\hat{q}_e^*} \boldsymbol{\xi}_d^b \times \boldsymbol{\xi}_e^b] \end{aligned} \quad (16)$$

where  $\hat{k}_p = \mathbf{k}_{pr} + \epsilon \mathbf{k}_{pd} = (k_{pr1}, k_{pr2}, k_{pr3})^T + \epsilon(k_{pd1}, k_{pd2}, k_{pd3})^T$ ,  $\hat{k}_d = \mathbf{k}_{dr} + \epsilon \mathbf{k}_{dd} = (k_{dr1}, k_{dr2}, k_{dr3})^T + \epsilon(k_{dd1}, k_{dd2}, k_{dd3})^T$ , and  $\hat{k}_i = \mathbf{k}_{ir} + \epsilon \mathbf{k}_{id} = (k_{ir1}, k_{ir2}, k_{ir3})^T + \epsilon(k_{id1}, k_{id2}, k_{id3})^T$ .

The stability of the system controlled by the PID feedback linearization tracker with respect to the desired position and attitude for almost all initial states is proved in the remainder of this subsection: Substituting (7) into (14) yields that

$$\dot{\boldsymbol{\xi}}_e^b = \hat{\mathbf{F}} - Ad_{\hat{q}_e^*} \dot{\boldsymbol{\xi}}_d^b - [\hat{0}, Ad_{\hat{q}_e^*} \boldsymbol{\xi}_d^b \times \boldsymbol{\xi}_e^b] + \hat{\mathbf{U}} \quad (17)$$

Combining (16) with (17) brings that

$$\dot{\boldsymbol{\xi}}_e^b = -2 \left( \hat{k}_p \cdot \ln \hat{q}_e + \hat{k}_i \cdot \int_0^t \ln \hat{q}_e dt + \hat{k}_d \cdot (\ln \hat{q}_e)' \right) \quad (18)$$

Therefore, in order to prove that the PID feedback linearization tracker can enable the tilt-rotor multi-rotor UAV to move stably along the desired position and attitude, we only need to prove that closed-loop system error dynamics is converging as time goes to infinity.

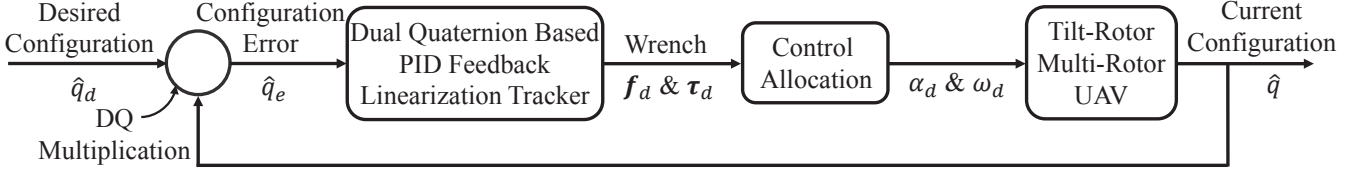


Fig. 2. Control structure for a tilt-rotor multi-rotor UAV.

Applying the definition of the logarithmic mapping to (18) obtains that

$$\begin{aligned}\dot{\epsilon}_e^b &= -\hat{k}_p \cdot (\theta_e^b + \epsilon p_e^b) - \hat{k}_i \cdot \int_0^t (\theta_e^b + \epsilon p_e^b) dt \\ &\quad - \hat{k}_d \cdot (\dot{\theta}_e^b + \epsilon \dot{p}_e^b) \\ &= \left[ 0, -K_{pr} \theta_e^b - K_{ir} \int_0^t \theta_e^b dt - K_{dr} \dot{\theta}_e^b \right] \\ &\quad + \epsilon \left[ 0, -K_{pd} p_e^b - K_{id} \int_0^t p_e^b dt - K_{dd} \dot{p}_e^b \right]\end{aligned}\quad (19)$$

where definitions of  $K_{pr}$ ,  $K_{ir}$ ,  $K_{dr}$ ,  $K_{pd}$ ,  $K_{id}$ , and  $K_{dd}$  are given in Section II-A.

Comparing (19) with (13) for both real part and dual part, we can observe that

$$\ddot{\theta}_e^b = -K_{pr} \theta_e^b - K_{ir} \int_0^t \theta_e^b dt - K_{dr} \dot{\theta}_e^b \quad (20)$$

$$\begin{aligned}\ddot{p}_e^b &= -K_{pd} p_e^b - K_{id} \int_0^t p_e^b dt - K_{dd} \dot{p}_e^b \\ &\quad - \dot{\theta}_e^b \times p_e^b - \dot{\theta}_e^b \times \dot{p}_e^b\end{aligned}\quad (21)$$

Applying Laplace transformation to (20) yields that

$$\begin{aligned}s^2 \Theta_e^b - s \Theta_e^b(0) - \dot{\Theta}_e^b(0) \\ = -K_{pr} \Theta_e^b - \frac{K_{ir}}{s} \Theta_e^b + \Theta_e^b(0) - s K_{dr} \Theta_e^b\end{aligned}\quad (22)$$

Rearranging (22), the expression for  $\Theta_e^b$  can be gotten as

$$\Theta_e^b = D_r^{-1} \left[ \Theta_e^b(0) s^2 + \left( \Theta_e^b(0) + \dot{\Theta}_e^b(0) \right) s \right] \quad (23)$$

where  $D_r = s^3 I + s^2 K_{dr} + s K_{pr} + K_{ir}$ . According to (23), the appropriate  $K_{pr}$ ,  $K_{ir}$ , and  $K_{dr}$  need to be found so that each root of  $D_r = 0$  is on the left half of the complex plane. Therefore, the Routh-Hurwitz criterion for stability is used to figure out the condition of the stability of the tilt-rotor multi-rotor UAV system. The conditions for the stability are  $K_{pr}$ ,  $K_{ir}$ ,  $K_{dr} > 0$  and  $K_{pr} K_{dr} > K_{ir}$ .

Then, we can make use of all forces from originated rotational velocity and acceleration to define

$$F(\dot{\theta}_e^b, \ddot{\theta}_e^b) = \ddot{\theta}_e^b \times p_e^b + \dot{\theta}_e^b \times \dot{p}_e^b \quad (24)$$

Combining the conclusion of (23) with the basis of the stability of (16), we can obtain that when  $t \rightarrow \infty$ ,  $\theta_e^b \rightarrow 0$ ,  $\dot{\theta}_e^b \rightarrow 0$ , and  $\ddot{\theta}_e^b \rightarrow 0$ , that is  $F(\dot{\theta}_e^b, \ddot{\theta}_e^b) \rightarrow 0$ . It means there is always a situation that after a certain finite time, the value of the function  $F(\dot{\theta}_e^b, \ddot{\theta}_e^b)$  becomes trivial. Therefore, (21) after this moment can be degenerated to

$$\ddot{p}_e^b = -K_{pd} p_e^b - K_{id} \int_0^t p_e^b dt - K_{dd} \dot{p}_e^b \quad (25)$$

Equation (25) has the similar form as (20). Thus, the conditions for the stability are similar as before, which are  $K_{pd}$ ,

$K_{id}$ ,  $K_{dd} > 0$  and  $K_{pd} K_{dd} > K_{id}$ . In conclusion, after satisfying two conditions:  $K_{pr}$ ,  $K_{ir}$ ,  $K_{dr}$ ,  $K_{pd}$ ,  $K_{id}$ ,  $K_{dd} > 0$  and  $K_{pr} K_{dr} > K_{ir}$  &  $K_{pd} K_{dd} > K_{id}$ , the tilt-rotor multi-rotor UAV controlled by (16) is stable.

After the required  $\hat{U}$  is obtained through the PID feedback linearization tracker, the desired forces and moments can be derived as follows:

$$\begin{cases} f_d = [\text{Du}(\hat{U}) - \text{Re}(\hat{U}) \times p^b] m \\ \tau_d = J \text{ Re}(\hat{U}) \end{cases} \quad (26)$$

where  $\text{Re}(\cdot)$  and  $\text{Du}(\cdot)$  are real and dual parts of the dual vector  $(\cdot)$ , respectively.

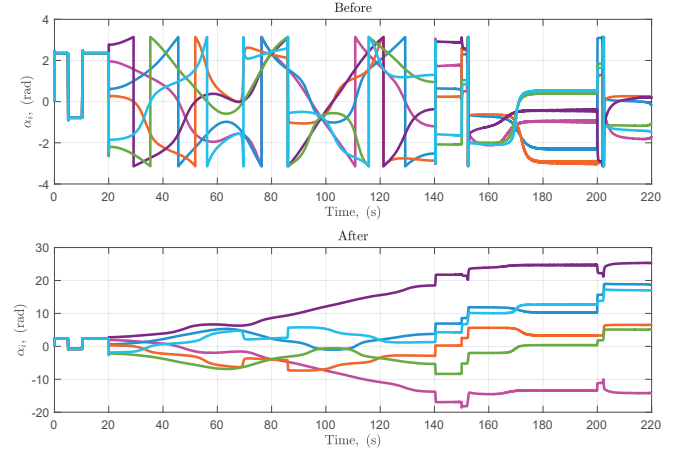


Fig. 3. Arm rotation angles,  $\alpha_i$ , with respect to time  $t$  before and after processed.

### C. Control Allocation

The relationship between the body force and torque with respect to squared rotor speeds,  $\tilde{\Omega}$ , is shown in (27) [1].

$$\begin{bmatrix} f \\ \tau \end{bmatrix} = A \tilde{\Omega} \quad A \in \mathbb{R}^{6 \times 2n}, \tilde{\Omega} \in \mathbb{R}^{2n} \quad (27)$$

where  $A$  is the static allocation matrix,  $n$  is the number of tilt arms,  $\alpha_i$  are the rotor orientations, and the lateral and vertical components of each squared rotor speed in the respective rotor unit frame are represented by the elements of the vector  $\tilde{\Omega}$ .

After the desired wrench-force  $f_d$  and moment  $\tau_d$ —is derived in (26), actuator commands—rotor speeds ( $\omega_i$ ) and rotor orientations ( $\alpha_i$ )—need to be determined using the aerodynamic model in (27). However, the system is underdetermined since the static allocation matrix  $A$  is irreversible. In this case, one of the generalized inverse matrices, the Moore-Penrose pseudo-inverse ( $A^\dagger$ ), can be utilized to calculate rotor speeds and orientations. The Moore-Penrose pseudo-inverse can obtain the

minimum norm solution of (27) as follows. This minimization of the norm not only reduces power consumption but also has characteristics of being more consistent and equally distributed angular velocities [2].

$$\tilde{\Omega} = A^\dagger \begin{bmatrix} f_d \\ \tau_d \end{bmatrix}, \quad A^\dagger \in \mathbb{R}^{2n \times 6} \quad (28)$$

Now, the value of each ingredient in  $\tilde{\Omega}$  is known. In this case, it is convenient to obtain the desired rotor speeds  $\omega_i$  and rotor orientations  $\alpha_i$  for each rotor, which can be done by solving (29).

$$\begin{cases} \omega_i = \sqrt[4]{\tilde{\Omega}_{2i-1}^2 + \tilde{\Omega}_{2i}^2} \\ \alpha_i = \text{atan2}(\tilde{\Omega}_{2i-1}, \tilde{\Omega}_{2i}) \end{cases}, i = 1, \dots, n \quad (29)$$

where  $\tilde{\Omega}_{(\cdot)}$  is the  $(\cdot)^{\text{th}}$  component of matrix  $\tilde{\Omega}$  and  $\text{atan2}(X, Y)$  represents the four-quadrant arctangent of the elements of  $X$  and  $Y$  such that  $-\pi \leq \text{atan2}(X, Y) \leq \pi$ .

**Algorithm 1:** Solve the singularity problem caused by using  $\text{atan2}(X, Y)$ .

---

```

 $\Delta\alpha_i \leftarrow \alpha_i^t - \alpha_i^{t-1};$ 
if  $\Delta\alpha_i \geq C$  then
     $\Delta\alpha_i = \text{sign}(\alpha_i^{t-1}) \cdot (\alpha_i^t + \alpha_i^{t-1});$ 
end
 $\alpha_i^{t*} = \alpha_i^{(t-1)*} + \Delta\alpha_i$ 

```

---

However, the singularity problem will occur if  $\alpha_i$  are obtained directly based on the above method. The upper figure of Fig. 3 shows the direct output curve of  $\alpha_i$  in certain simulation cases, from which it can be observed that the values of  $\alpha_i$  are discontinuous near  $\pi$  and  $-\pi$ . This is because the range of function,  $\text{atan2}(X, Y)$ , is limited between  $-\pi$  and  $\pi$ . The singularity of  $\alpha_i$  is detrimental for both the analysis of the tilting process of the rotors and the execution of the motors. A simple approach is demonstrated by the algorithm logic diagram of its basic idea in Algorithm 1. In this algorithm,  $\alpha_i^t$  is the input arm rotation angles  $\alpha_i$  at time  $t$  calculated by  $\text{atan2}(X, Y)$ ,  $\alpha_i^{t*}$  is the output arm rotation angles after processed,  $C$  is the maximum tolerance for the difference of

the arm rotation angles between each step, and  $\text{sign}(\cdot)$  is a function to judge the sign of  $(\cdot)$ . The  $\alpha_i$  obtained after conducting the process of solving the singularity problem is shown in the lower figure of Fig. 3.

#### IV. SIMULATION STUDIES

In this section, the PID feedback linearization tracker designed in Section III is implemented with the tilt-rotor hex-rotor UAV to simulate the position and attitude tracking performance. Two cases are performed to demonstrate how the PID feedback linearization tracker works for the trajectory tracking and the robustness to the disturbance. The system parameters of the tilt-rotor hex-rotor UAV in [1] are adopted here, which are shown in the following tabular.

$$\begin{aligned} m &= 4.27 \text{ kg} & J &= \text{diag}(0.086, 0.088, 0.16) \text{ kg} \cdot \text{m}^2 \\ d &= 0.83 \text{ m} & c_f &= 7.1 \times 10^{-6} \text{ N} \cdot \text{s}^2/\text{rad}^2 \\ l_x &= 0.415 \text{ m} & c_d &= 0.415 \text{ N} \cdot \text{s}^2/\text{rad}^2 \\ l &= 0.3 \text{ m} & \beta &= 0.6154 \cdot [1 \ -1 \ 1 \ -1 \ 1 \ -1] \\ C &= 5 & \gamma &= \frac{\pi}{3}i - \frac{\pi}{6}, i = 1, \dots, 6 \end{aligned}$$

The control gains of the PID feedback linearization tracker for the tilt-rotor hex-rotor UAV are listed in (30).

$$\begin{cases} \hat{k}_p = [5, 5, 5]^T + \epsilon [5, 5, 5]^T \\ \hat{k}_i = [0.1, 0.1, 0.1]^T + \epsilon [0.1, 0.1, 0.1]^T \\ \hat{k}_d = [10, 10, 10]^T + \epsilon [10, 10, 10]^T \end{cases} \quad (30)$$

##### A. Case I: Trajectory Tracking

In this subsection, to validate the effectiveness of the proposed controller, the control objective is to drive the tilt-rotor hex-rotor UAV to follow the predefined omnidirectional trajectory. The desired motion trajectory and orientation are designed as: the UAV rises 5 meters from the starting point for  $t \in [0, 10]$  s and hovers from 10 to 20 seconds. After 20 second, the UAV is tracking along a three-dimensional figure- $\infty$  shape. The desired trajectory after 20 second is

$$\begin{cases} p_d^s = 5 [\sin 2T, \sin T, 1 - \cos 2T] \text{ m} \\ \theta_d^s = [0, Tn] \end{cases} \quad (31)$$

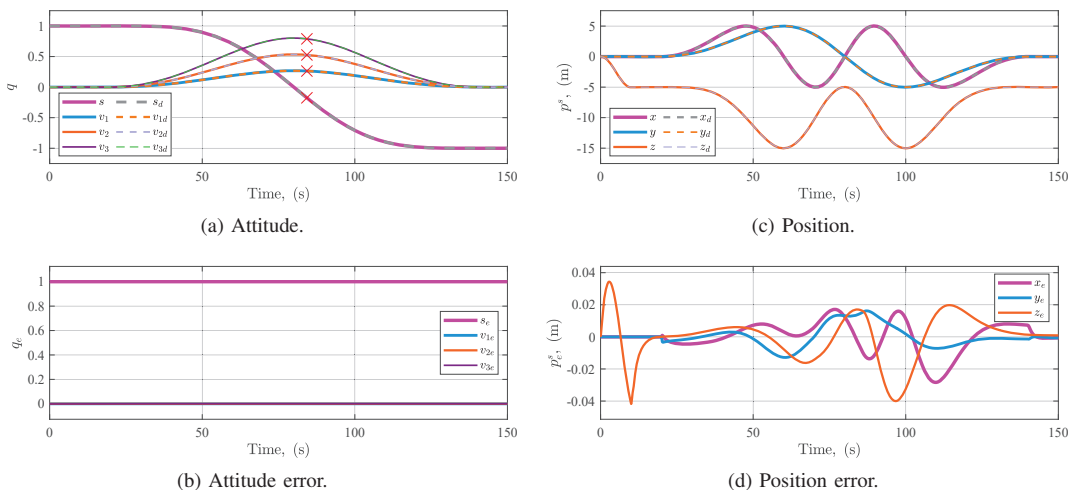


Fig. 4. Case I. Trajectory tracking - solid lines are actual trajectory, dashed lines are desired trajectory, and four red  $\times$  marks represent the case where singularity occurs if the system is described by Euler angles (roll =  $\pi$ ).

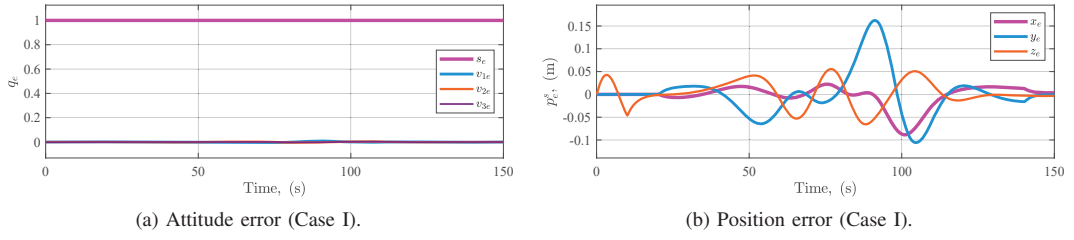


Fig. 5. Case I. Trajectory tracking - Tracking errors for the PD controller in [20].

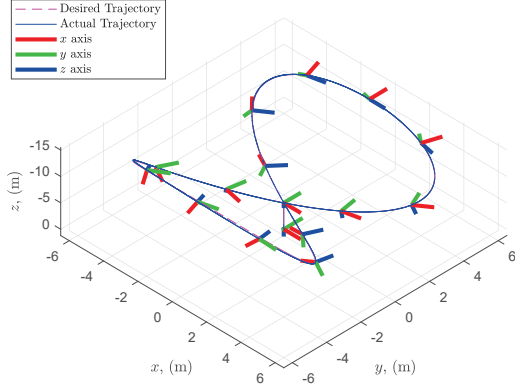


Fig. 6. Motion trajectory of the tilt-rotor hex-rotor UAV.

where

$$T = \begin{cases} \pi [1 - \cos \frac{\pi}{120} (t - 20)] & t \in [20, 140] \text{ s} \\ 0 & t \in [140, \infty) \end{cases} \quad (32)$$

and  $n = [1, 2, 3]$ . The role of  $T$  here is to make the acceleration and angular acceleration of the UAV be 0 when  $t = 0$  s,  $t = 10$  s,  $t = 20$  s and  $t = 140$  s, thus leading the entire trajectory to be smoother.

With the trajectory set up above, the results gotten from the PID feedback linearization tracker are shown in Fig. 4. Fig. 4 (a) demonstrates the development of four elements of the actual orientation  $q$  with regard to time  $t$ . In this figure, the four red  $\times$  marks represent the case where singularity occurs if the system is described by Euler angles. Fig. 4 (c) shows the development of three elements of the actual position  $p^s$  with regard to time  $t$ . From Fig. 4 (a) and (c), it can be shown that the proposed controller is effective as it can drive the tilt-rotor multi-rotor UAV to accurately follow the desired omnidirectional trajectory. Besides, the singularity occurs at the time  $t = 84.9$  s if the system is described by the Euler angle representation as marked in Fig. 4 (a). This discontinuity will cause the phenomenon called unwinding, where the feedback unnecessarily rotates the rigid body up to a full rotation [27]. Hence, it can be seen that the controller based on dual quaternion can continuously generate the proper control commands without causing discontinuity problems. The errors of attitude and position are shown in Fig. 4 (b) and (d), respectively. To better show the superiority of the proposed PID feedback linearization tracker, the comparison with the PD controller in [20] is carried out:

$$\begin{aligned} \hat{U} = & -2\hat{k}_p \cdot \ln \hat{q}_e - \hat{k}_d \cdot \xi_e^b - \hat{F} \\ & + Ad_{\hat{q}_e^*} \dot{\xi}_d^b + [\hat{0}, Ad_{\hat{q}_e^*} \xi_d^b \times \xi_e^b] \end{aligned} \quad (33)$$

The controller parameters are tuned to achieve the best possible performance as  $\hat{k}_p = [2, 2, 2]^T + \epsilon [2, 2, 2]^T$  and  $\hat{k}_d = [5, 5, 5]^T + \epsilon [5, 5, 5]^T$  and the simulation results are plotted in Fig. 5. For the same case, the tracking error for the PID tracker is smaller than that of the PD tracker. Furthermore, the 3D motion trajectory in the aforementioned case for the proposed PID controller is also plotted in Fig. 6. The statistics of simulation results, including, maximum, mean and RMSE, for both PID and PD controllers are shown in Table I.

#### B. Case II: Robustness to Disturbance

In this subsection, the robustness of our proposed PID feedback linearization tracker to two types of disturbances, i.e., impulse disturbance, which simulates sudden impact, such as bird strike and sinusoidal disturbance, which simulates continuous environmental interference, such as wind, is tested. The PD controller from [20] is also used for comparison purposes without changing the controller parameter. The parameters of the proposed controller are also the same as Case I. The UAV is initially hovering at  $\hat{q} = [1, 0, 0, 0] + \epsilon [0, 0, 0, 0]$  and the impulse disturbance test is carried out by applying a disturbance force of 1 N \$\cdot\$ m from 5 to 7 seconds and a disturbance torque of 5 N from 20 to 22 seconds in each of  $x$ -,  $y$ -, and  $z$ - directions. The sinusoidal disturbance test is performed by applying a time-varying disturbance torque of  $\sin 0.2\pi t$  N \$\cdot\$ m and a time-varying disturbance force of  $5 \sin 0.2\pi t$  N in each of  $x$ -,  $y$ -, and  $z$ - directions from  $t = 0$  s. The irregular disturbance test is performed by applying a time-varying disturbance torque of  $(0.2 \sin 0.2\pi t + 0.2 \sin 0.3\pi t)$  N \$\cdot\$ m and a time-varying disturbance force of  $(\sin 0.2\pi t + \sin 0.3\pi t)$  N in each of  $x$ -,  $y$ -, and  $z$ - directions from  $t = 0$  s. The simulation results are shown in Fig. 7. From Figs. 7 (a) and (d), it can be seen that the designed PID feedback linearization tracker can enable tilt-rotor multi-rotor UAVs with strong robustness to impulse disturbances. Even though it has a limitation that when the system suffers from a force equivalent to 1.2 times the self-gravity of the system, the system will diverge, the overall controllability and stability of the system are effective. Moreover, when the system is subjected to the time-varying disturbance, the system controlled by PID feedback linearization tracker has better robustness than that of PD tracker, as shown in Fig. 8. The statistics of the simulation results, including, maximum, mean and RMSE are shown in Table. I.

#### V. CONCLUSIONS

In this paper, a novel PID feedback linearization tracker based on the unit dual quaternion for tilt-rotor multi-rotor

TABLE I. Comparison between PID and PD tracker: maximum represents the maximum value of error, mean indicates the average value of the overall error, and RMSE is the root mean square error.

Case	Error parameter	PID tracker		PD tracker	
		Position, (m)	Attitude, (rad)	Position, (m)	Attitude, (rad)
I	Maximum	0.0694	0.0050	0.1683	0.0138
	Mean	0.0102	0.0008	0.0532	0.0466
	RMSE	0.0166	0.0015	0.0839	0.0656
II (impulse)	Maximum	0.1686	2.1360	0.2135	3.1120
	Mean	0.0129	0.1164	0.0123	0.1002
	RMSE	0.0358	0.3431	0.0413	0.3823
II (regular)	Maximum	0.0525	0.2229	0.0743	0.6345
	Mean	0.0062	0.0641	0.0183	0.2278
	RMSE	0.0082	0.0799	0.0168	0.2625
II (irregular)	Maximum	0.0098	0.0235	0.0722	0.2792
	Mean	0.0000	0.0001	0.0005	0.0011
	RMSE	0.0049	0.0106	0.0316	0.0826

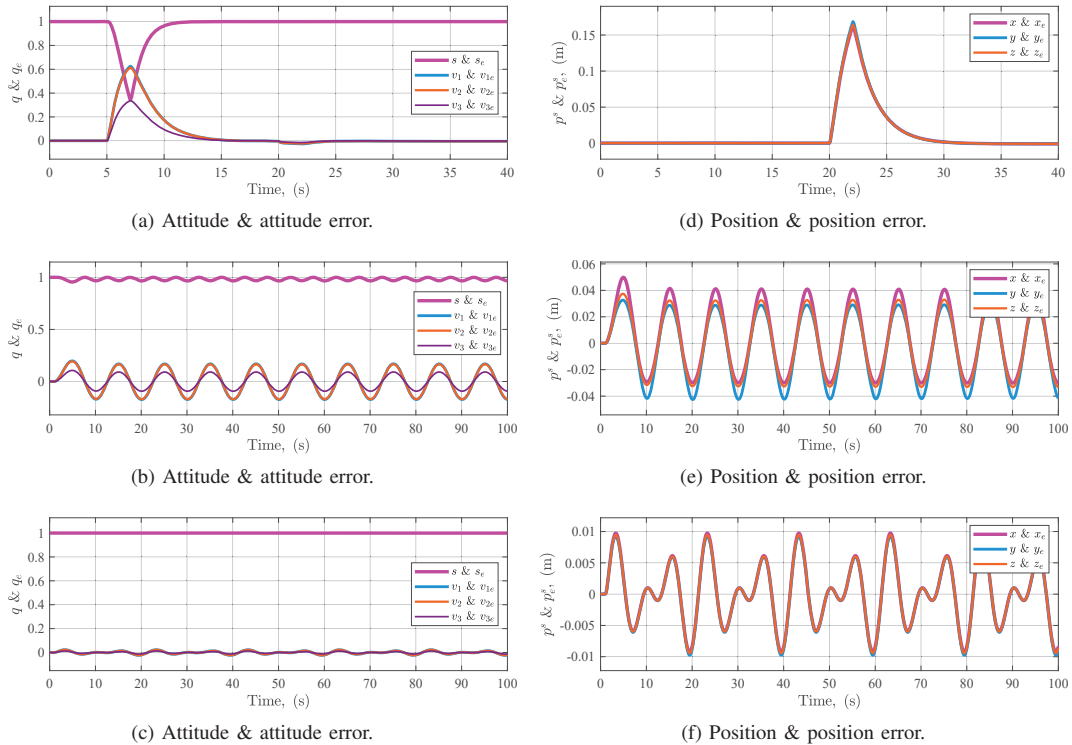


Fig. 7. Case II. Robustness to disturbance. First row: impulse disturbance; second row: sinusoidal disturbance; third row: irregular disturbance.

UAVs has been designed. This PID feedback linearization tracker can couple kinematics and dynamics analysis of the tilt-rotor multi-rotor UAV platform for both translational and rotational motion and eliminate singularity problems existing on the Euler angle. After proving the stability of the PID feedback linearization tracker we designed, we utilized it on the tilt-rotor hex-rotor UAV platform to verify the feasibility and superiority of this tracker. The results exemplified that this PID feedback linearized tracker exploits the mathematical simplicity of the unit dual quaternion and its exponential mapping to control stably tilt-rotor multi-rotor UAV using simple state feedback. In the future, the control allocation needs to be enhanced under some special cases and motor control also needs to be designed. After these, the PID

feedback linearization tracker will be applied to the actual tilt-rotor multi-rotor UAV platform to bring our project to further fruition.

## REFERENCES

- [1] M. Allenspach, K. Bodie, M. Brunner, L. Rinsoz, Z. Taylor, M. Kamel, R. Siegwart, and J. Nieto, "Design and optimal control of a tiltrotor micro-aerial vehicle for efficient omnidirectional flight," *The International Journal of Robotics Research*, vol. 39, no. 10-11, pp. 1305–1325, 2020.
- [2] M. Kamel, S. Verling, O. Elkhattib, C. Sprecher, P. Wulkop, Z. Taylor, R. Siegwart, and I. Gilitschenski, "The voliro omniorientational hexacopter: An agile and maneuverable tilttable-rotor aerial vehicle," *IEEE Robotics & Automation Magazine*, vol. 25, no. 4, pp. 34–44, 2018.
- [3] M. Brunner, K. Bodie, M. Kamel, M. Pantic, W. Zhang, J. Nieto, and R. Siegwart, "Trajectory tracking nonlinear model predictive control for an overactuated MAV," in *2020 IEEE International Conference on Robotics and Automation (ICRA)*. IEEE, 2020, pp. 5342–5348.

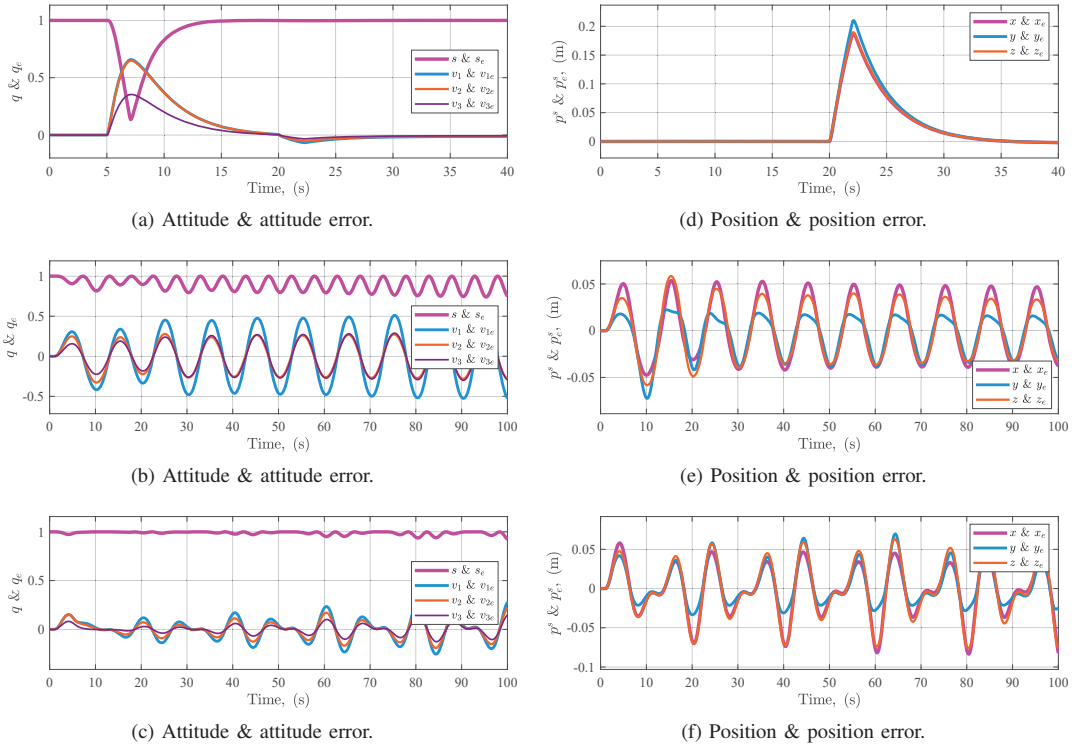


Fig. 8. Case II. Robustness to disturbance - Tracking errors for the PD controller in [20]. First row: impulse disturbance; second row: sinusoidal disturbance; third row: irregular disturbance.

- [4] W. Zhang, M. Brunner, L. Ott, M. Kamel, R. Siegwart, and J. Nieto, “Learning dynamics for improving control of overactuated flying systems,” *IEEE Robotics and Automation Letters*, vol. 5, no. 4, pp. 5283–5290, 2020.
- [5] S. Sridhar, R. Kumar, G. Gupta, M. Kumar, and K. Cohen, “Nonlinear control of a novel class of tilt-rotor quadcopters using sliding mode method: Theory and hardware implementation,” *Journal of Aerospace Engineering*, vol. 35, no. 3, p. 04022017, 2022.
- [6] A. AlAttar and P. Kormushev, “Kinematic-model-free orientation control for robot manipulation using locally weighted dual quaternions,” *Robotics*, vol. 9, no. 4, p. 76, 2020.
- [7] G. Günaşti, “Quaternions algebra, their applications in rotations and beyond quaternions,” B.S. Thesis, School of Computer Science, Linnaeus University, 2012.
- [8] L. Perumal, “Quaternion and its application in rotation using sets of regions,” *International Journal of Engineering and Technology Innovation*, vol. 1, no. 1, pp. 35–52, 2011.
- [9] Y. Wang and R. Rajamani, “Direction cosine matrix estimation with an inertial measurement unit,” *Mechanical Systems and Signal Processing*, vol. 109, pp. 268–284, 2018.
- [10] A. Prach and E. Kayacan, “An MPC-based position controller for a tilt-rotor tricopter VTOL UAV,” *Optimal control applications and methods*, vol. 39, no. 1, pp. 343–356, 2018.
- [11] R. Kumar, S. R. Agarwal, and M. Kumar, “Modeling and control of a tethered tilt-rotor quadcopter with atmospheric wind model,” *IFAC-PapersOnLine*, vol. 54, no. 20, pp. 463–468, 2021.
- [12] R. Chiappinelli, M. Cohen, M. Doff-Sotta, M. Nahon, J. R. Forbes, and J. Apkarian, “Modeling and control of a passively-coupled tilt-rotor vertical takeoff and landing aircraft,” in *2019 International Conference on Robotics and Automation (ICRA)*. IEEE, 2019, pp. 4141–4147.
- [13] A. Nikhilraj, H. Simha, and H. Priyadarshan, “Modeling and control of port dynamics of a tilt-rotor quadcopter,” *IFAC-PapersOnLine*, vol. 55, no. 1, pp. 746–751, 2022.
- [14] J. Cenesa, A. Pérez-Navarro, J. Sospedra, and R. Montoliu, *Geographical and Fingerprinting Data to Create Systems for Indoor Positioning and Indoor/Outdoor Navigation*. Elsevier, 2018.
- [15] R. Falconi and C. Melchiorri, “Dynamic model and control of an overactuated quadrotor UAV,” *IFAC Proceedings Volumes*, vol. 45, no. 22, pp. 192–197, 2012.
- [16] R. Kumar, M. Bhargavapuri, A. M. Deshpande, S. Sridhar, K. Cohen, and M. Kumar, “Quaternion feedback based autonomous control of a quadcopter UAV with thrust vectoring rotors,” in *2020 American Control Conference (ACC)*. IEEE, 2020, pp. 3828–3833.
- [17] Y. T. Yeo and H. H. Liu, “Transition control of a tilt-rotor VTOL UAV,” in *2018 AIAA Guidance, Navigation, and Control Conference*, 2018, p. 1848.
- [18] J. T. VanderMey, “A tilt rotor UAV for long endurance operations in remote environments,” Ph.D. dissertation, Department of Aeronautics and Astronautics, Massachusetts Institute of Technology, 2011.
- [19] X. Wang and C. Yu, “Unit-dual-quaternion-based PID control scheme for rigid-body transformation,” *IFAC Proceedings Volumes*, vol. 44, no. 1, pp. 9296–9301, 2011.
- [20] —, “Unit dual quaternion-based feedback linearization tracking problem for attitude and position dynamics,” *Systems & Control Letters*, vol. 62, no. 3, pp. 225–233, 2013.
- [21] J. Carino, H. Abaunza, and P. Castillo, “Quadrotor quaternion control,” in *2015 International Conference on Unmanned Aircraft Systems (ICUAS)*. IEEE, 2015, pp. 825–831.
- [22] H. Abaunza, J. Carino, P. Castillo, and R. Lozano, “Quadrotor dual quaternion control,” in *2015 Workshop on Research, Education and Development of Unmanned Aerial Systems (RED-UAS)*. IEEE, 2015, pp. 195–203.
- [23] W. K. Clifford, *Mathematical papers*. American Mathematical Society, 2007.
- [24] J. Gallier, *Geometric methods and applications: for computer science and engineering*. Springer Science & Business Media, 2011.
- [25] X. Wang, D. Han, C. Yu, and Z. Zheng, “The geometric structure of unit dual quaternion with application in kinematic control,” *Journal of Mathematical Analysis and Applications*, vol. 389, no. 2, pp. 1352–1364, 2012.
- [26] H. Wong, H. Pan, and V. Kapila, “Output feedback control for spacecraft formation flying with coupled translation and attitude dynamics,” in *2005 American Control Conference (ACC)*. IEEE, 2005, pp. 2419–2426.
- [27] C. G. Mayhew, R. G. Sanfelice, and A. R. Teel, “On quaternion-based attitude control and the unwinding phenomenon,” in *2011 American Control Conference (ACC)*. IEEE, 2011, pp. 299–304.